NIOBIUM IN HEAVY AND MEDIUM SECTIONS FOR HIGH-RISE STRUCTURES

D. Misra[1] and S.G. Jansto[2]

[1]Center for Structural and Functional Materials,
University of Louisiana at Lafayette, Lafayette, LA 70504-4130, USA
[2]CBMM North America, Inc., 1000 Old Pond Road,
Bridgeville, PA 15017, USA

Keywords: Steel Sections, Niobium, Microalloyed Steel, Precipitation, Degenerate Pearlite, Microstructure, Mechanical Properties, Charpy Toughness, TEM

Abstract

In view of the recent demand for heavy and medium sections for high-rise structures, the Nb-microalloying approach is being increasingly considered for the production of these steel shapes with improved mechanical properties. This paper provides a metallurgical background, with focus on processing-microstructure-property relationships, illustrating that high strength in heavy and medium sections with the desired strength-toughness combination can be successfully obtained by the effective use of an Nb-microalloying approach.

Background

There is currently a demand for heavy sections with superior yield strength approaching ~450 MPa and a minimum impact toughness of 34 J (~25 ft-lb) at ~4.5 °C (40 °F). This demand is dictated by extreme weather conditions and seismic requirements. The objective of the present paper is to address the attractive nature of Nb in the production of heavy and medium beam sections, with particular focus on the microstructure-property relationship. The objectives of adding Nb to steels are diverse and include:

i. Combine and pin N within the steel, thereby decreasing the free N content for the benefit of toughness [1];
ii. Prevent austenite recrystallization and/or grain growth during processing [2];
iii. Control of austenite grain size;
iv. Lower austenite-ferrite transformation temperature, retarding ferrite formation in microalloyed steels;
v. Refine polygonal ferrite grains during transformation;
vi. Precipitation hardening.

In the production of high strength low alloy steels, several of the above effects may operate simultaneously or individually. The magnitude of each effect varies proportionately with the Nb content and depends on the thermomechanical processing route.

Over 50% of the structural plate and beam sections have intermediate C levels ranging from 0.15 to 0.22%. There is a gradual shift at some mills, seeking participation in the value added structural plate and beam segment, to Nb-bearing structural grades at less than 0.10%C in order to transition to lower C base alloys for both plate and some long product applications. The benefits are not only improved mechanical properties and functional performance, but also the opportunity to reduce overall steelmaking cost per tonne through improved productivity, reduced diverts and improved product quality [3].

Excellent research and development progress has resulted in the successful commercialization of lower C, Nb-bearing microalloyed plate steel and near-net shape cast and rolled beams throughout the world. Many of these progressive metallurgical accomplishments are presented within this text. With increasing raw material and energy costs, the effects of processing parameters such as reheating temperature and cooling rate after hot rolling to achieve improved mechanical properties can result in significant savings. A lower total cost of production may be achieved through a low-C low-alloy (LCLA©) chemistry with selective accelerated cooling and better control of reheat furnace temperatures [3].

The strength is enhanced by the addition of Nb because of the cumulative contribution of refinement in grain size and precipitation of NbC in the ferrite grains. Figure 1 schematically illustrates the effect of Nb addition on grain refinement and increment in yield strength in steels. Nb offers advantages via a pinning effect on the austenite grain size and a widening of the temperature range for austenite processing [4]. Niobium nitrides or carbonitrides impede the coarsening of the austenite grains in a manner similar to aluminum nitrides. This effect is important to ensure a fine microstructure. The sluggish nature of recrystallization in Nb-treated steels results in pancake-shaped austenite grains leading to significant ferrite or bainite grain refinement in the final product.

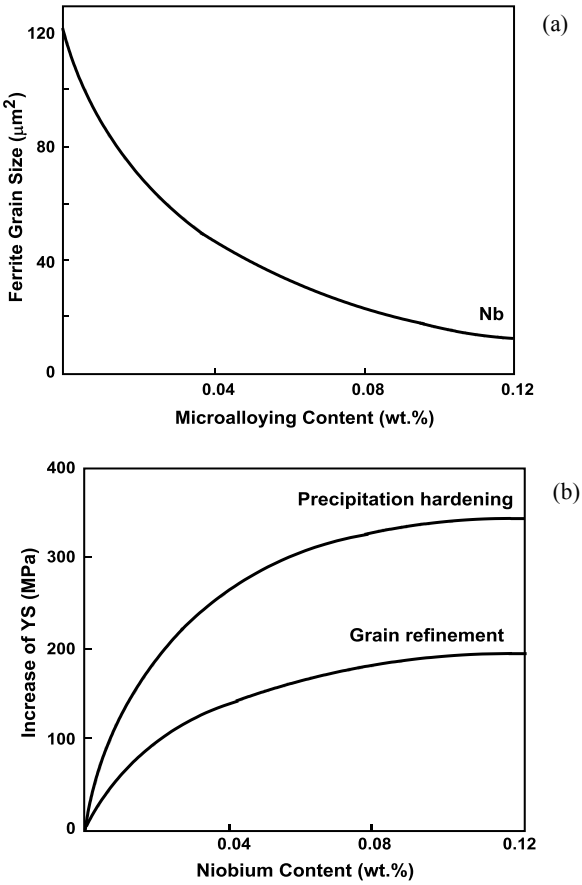

Figure 1. Influence of Nb on grain size area (a) and mechanical properties (b) of microalloyed steels [4].

The choice of Nb as a microalloying element is because of precipitation hardening and refinement of microstructure that gives a combination of high yield strength and increased toughness. The combined microalloying effect with Ti may exhibit a reduced hardening due to interaction of TiN precipitates with Nb [4].

In low C bainitic steels, Nb along with Mn and Mo is effective in increasing the volume fraction of bainite and this increases both yield and tensile strength. Figure 2 shows the effect of Nb on the strength and toughness properties of MoNi-steel plate of 20 mm thickness [5]. In bainitic plates, the primary microstructure is polygonal ferrite and granular bainite, while the secondary

constituents include martensite and retained austenite. The increase in Nb content was observed to increase the granular bainite fraction and refine the second phase constituents.

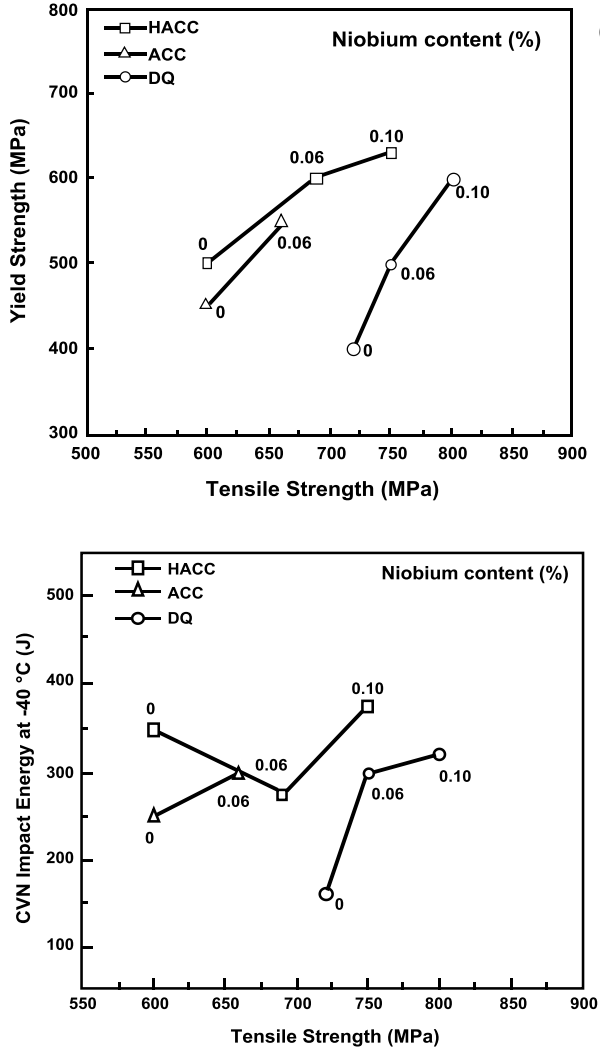

Figure 2. Effect of Nb and cooling on tensile (a) and toughness (b) properties of MoNi-steel plate of 20 mm thickness. (HACC: Heavy Accelerated Cooling, ACC: Accelerated Cooling, DQ: Direct Quenching) [5].

Nb for Heavy and Medium Sections

The footprint and significant advantages of Nb-microalloying in heavy and medium sections have been outlined [6]. The chemical compositions of commercially produced Nb-microalloyed steels fall within the ranges shown in Table I. The composition range outlined in Table I corresponds to the ASTM specification. It may be noted that the Nb content required to obtain the desired yield strength of 57-65 ksi in heavy and medium sections is generally in the range of ~0.02-0.04 wt.%.

Table I. Chemical Composition Range of Nb-microalloyed Steels

Elements	Nb-microalloyed steel (wt.%)
C	0.030-0.100
Mn	0.500-1.500
V	0.001
Nb	0.020-0.050
Si	0.15-0.25
P	0.010-0.020
S	0.015-0.025
N	0.009-0.010

Tensile and Impact Behavior of Nb-microalloyed Steels

Tensile property data for Nb-microalloyed steels are listed in Table II. Based on the chemistry, yield strengths of ~65 ksi and elongations of greater than 20% can be obtained with Nb as a microalloying element. However, Charpy V-notch impact toughness is a function of cooling rate through transformation (Figure 3) and is governed by the final microstructure (ie. ferrite-pearlite, degenerate pearlite or bainitic ferrite).

Table II. Representative Room Temperature Tensile Properties of Nb-microalloyed Steels

Properties	Nb-microalloyed Steels
Yield Strength (ksi)	57–65
Tensile Strength (ksi)	72–75
% Elongation	23–25

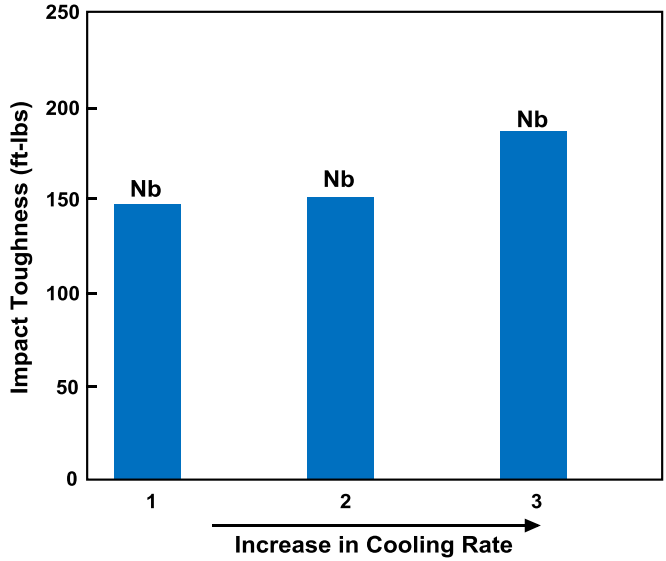

Figure 3. Room temperature Charpy V-notch impact toughness of Nb-microalloyed steels [6].

Microstructure of Nb-microalloyed Steels

Representative low and high magnification scanning electron micrographs of Nb-microalloyed steels processed at different cooling rates are presented in Figures 4-6. The primary microstructural constituents at low cooling rate are polygonal ferrite and pearlite. At intermediate cooling rate, the microstructure consisted of degenerate pearlite plus conventional pearlite, whereas at high cooling rates there was an increased tendency towards the formation of lath ferrite/bainitic ferrite with a consequent decrease in conventional ferrite-pearlite content. The microstructural transformation from low to intermediate to high cooling rate can be summarized as ferrite-pearlite→ferrite-degenerate pearlite→bainitic ferrite. Thus, the ultimate microstructure strongly determines the toughness in the final product.

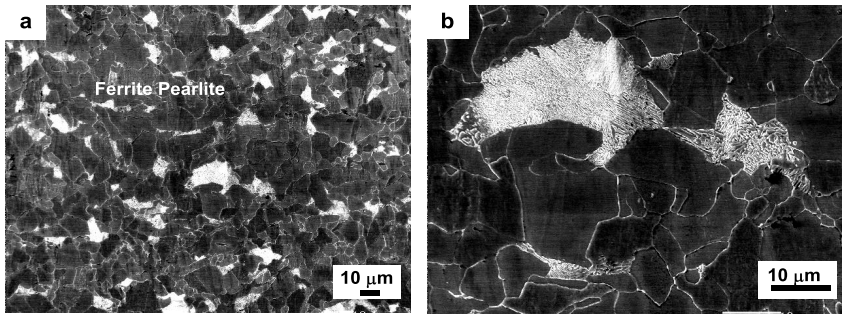

Figure 4. Representative; (a) low and (b) high magnification scanning electron micrographs of Nb-microalloyed steels processed at low cooling rate.

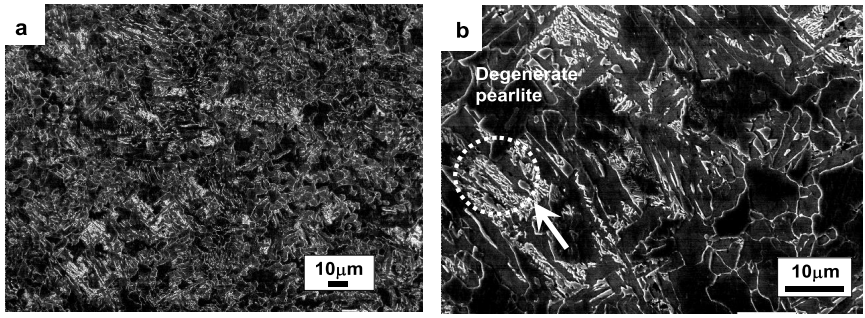

Figure 5. Representative; (a) low and (b) high magnification scanning electron micrographs of Nb-microalloyed steels processed at intermediate cooling rate. The micrograph (b) shows degenerate pearlite [6].

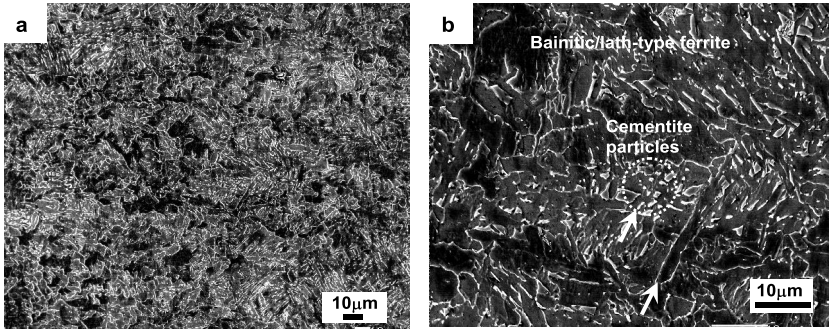

Figure 6. Representative; (a) low and (b) high magnification scanning electron micrographs illustrating the microstructure in Nb-microalloyed steels processed at high cooling rate [6].

In Figures 7-9, representative bright field TEM micrographs, summarizing the microstructure of Nb-microalloyed steels at low, intermediate and high cooling rates are presented. It may be seen that for the steel processed at low cooling rate (Figures 7(a-c)), the microstructure comprises of polygonal ferrite having coarse and fine grain size distributions (Figures 7(b-c)). At intermediate cooling rate, the microstructure consisted of elongated ferrite grains (Figure 8(a)) and also some coarse grains with high dislocation density (Figures 8(b-c)). At high cooling rate the microstructure predominantly contained lath-type or bainitic ferrite (Figures 9(a-c)). The different types of ferrite morphology are a consequence of different operating mechanisms [7,8]. The majority of the ferrite laths are oriented along a particular direction with the occasional presence of discontinuous cementite layers between them. If the driving force for the transformation is the reduction in C content, then the austenite is most likely to transform to lath-type ferrite by a shear mechanism at temperatures greater than 350 °C [7].

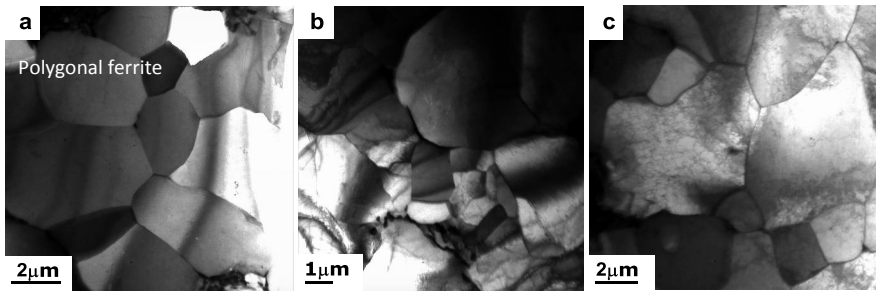

Figure 7. Bright field TEM micrographs of Nb-microalloyed steels illustrating the microstructure obtained at low cooling rate; (a, b) polygonal ferrite structure and (c) dislocation substructure in ferrite [6].

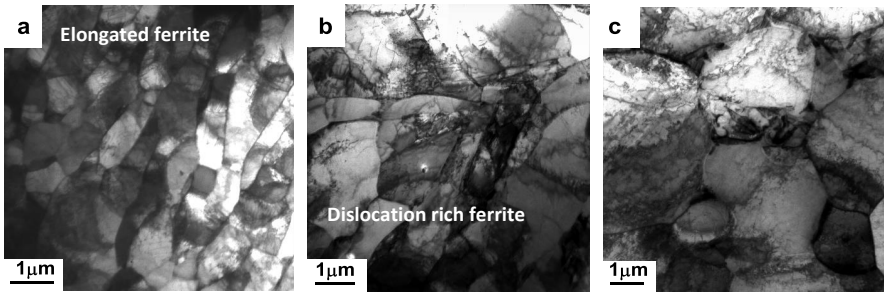

Figure 8. Bright field TEM micrographs of Nb-microalloyed steels illustrating the microstructure obtained at intermediate cooling rate; (a, b) elongated ferrite structure and (c) dislocation substructure in ferrite [6].

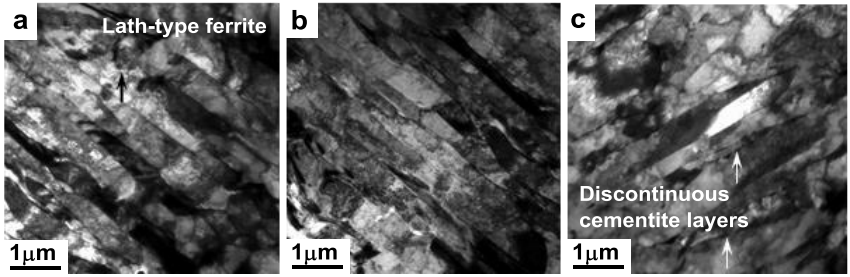

Figure 9. Bright field TEM micrographs of Nb-microalloyed steels illustrating the microstructure obtained at high cooling rate; (a, b and c) Bainitic/lath-type ferrite structure [6].

Representative bright field TEM micrographs of pearlite microstructures of Nb-microalloyed steels obtained at low, intermediate, and high cooling rates are presented in Figures 10-12 respectively. With an increase in cooling rate, the cementite morphology in the pearlite changes from lamellar pearlite to degenerate pearlite, and finally to small cementite particles. The steel processed at low cooling rate (Figures 10(a-b)) contains lamellar pearlite and broken lamellae (Figure 10(c)). At intermediate cooling rate some degenerate pearlite is also observed (Figures 11(a-b)). The SAD (selected area diffraction) pattern analysis of degenerate pearlite (Figure 11(b)) is presented in Figure 11(c).

Degenerate pearlite is formed by nucleation of cementite at the ferrite/austenite interface followed by carbide-free ferrite layers enclosing the cementite particles, in the transformation temperature range between normal pearlite and upper bainite [9]. A schematic diagram illustrating the mechanism of formation of degenerate pearlite is presented in Figure 12. Similar to lamellar pearlite, degenerate pearlite is also formed by a diffusion process and considering its morphology, the difference is attributed to insufficient C diffusion to develop continuous lamellae [7]. It is reported that the interface between ferrite and cementite in degenerate pearlite is wider than for the conventional pearlite, thus the interfacial grain boundary area in the controlled-rolled steels that contained degenerate pearlite is higher compared to the conventionally processed steel [10]. Degenerate pearlite enhances toughness [10] as discussed later in the paper.

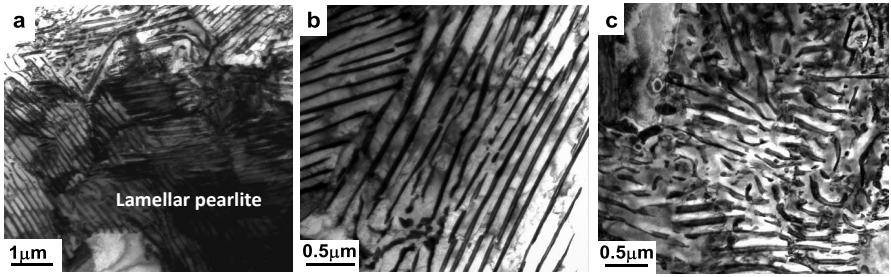

Figure 10. Bright field TEM micrographs of Nb-microalloyed steels illustrating the nature of pearlite obtained at low cooling rate; (a, b) lamellar pearlite structure and (c) broken-lamellae pearlite structure [6].

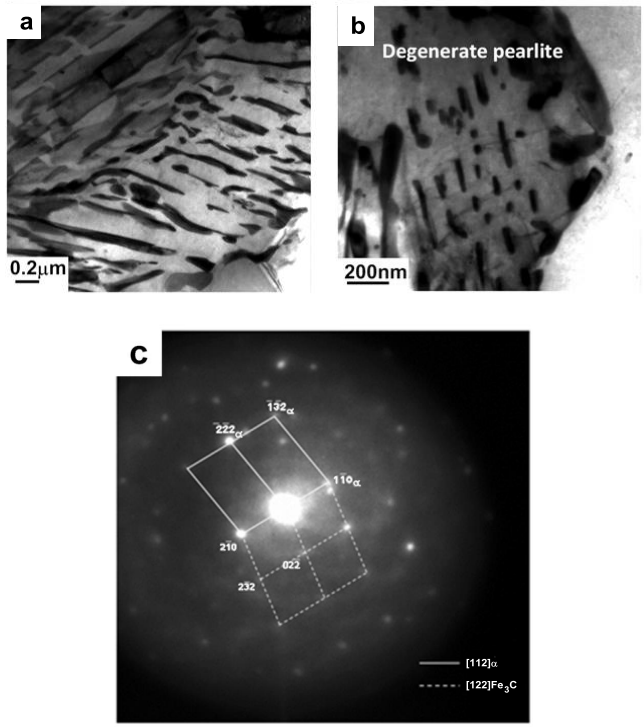

Figure 11. Bright field TEM micrographs of Nb-microalloyed steels illustrating the microstructure obtained at intermediate cooling rate; (a, b) degenerate pearlite and (c) SAD pattern analysis for image in (b) [6].

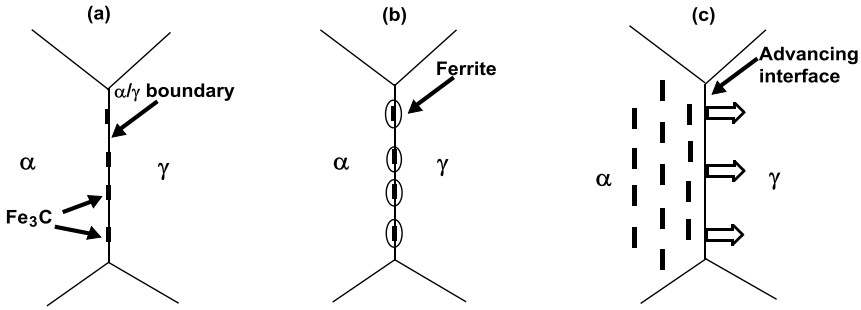

Figure 12. Schematic diagram illustrating the formation mechanism of degenerate pearlite.

At high cooling rate, the microstructure predominantly contained cementite particles dispersed in a ferrite matrix (Figures 13(a-b)) and at ferrite boundaries, (Figure 13(c)) of size range ~60-120 nm. The driving force for cementite spheroidization is a reduction in the interfacial area between the cementite lamellae and ferrite matrix [11,12]. The C content of ferrite in equilibrium with cementite is higher at the fragmented ends of cementite, ie. of high interfacial curvature, than the areas of low interfacial curvature. Hence, the spheroidization or formation of small particles is attributed to C diffusion through a ferrite matrix from regions of small radius of curvature to regions of large radius of curvature [11,12].

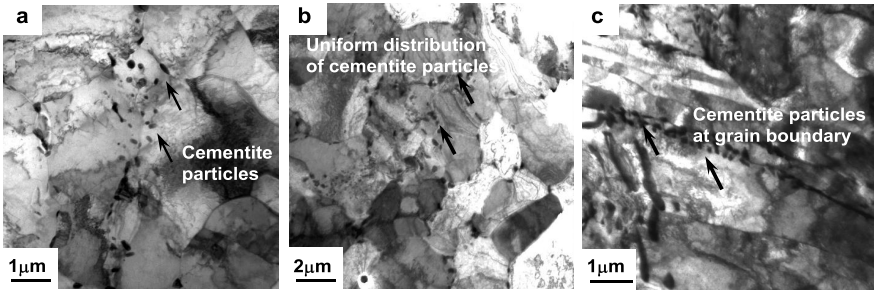

Figure 13**.** Bright field TEM micrographs of Nb-microalloyed steels processed at high cooling rate showing; (a) cementite particles in ferrite, (b) distribution of cementite particles in ferrite and (c) cementite particles at the ferrite grain boundary [6].

Precipitation in Nb-microalloyed Steels

Figures 14(a,b) show grain boundary precipitation and precipitation on dislocations in the ferrite region in Nb-microalloyed steels, while Figure 15(a) shows precipitation in the ferrite matrix together with the corresponding selected area diffraction (SAD) pattern in Figure 15(b). The SAD pattern analysis indicated that the fine precipitates were MC type cubic niobium carbides and the precipitates exhibited a $[100]_{\alpha}//[110]_{NbC}$ Baker-Nutting orientation relationship with the ferrite matrix. The characteristics of the precipitates in terms of mean particle size, mean inter-particle spacing and particle density in the matrix of Nb-microalloyed steels are summarized in Table III.

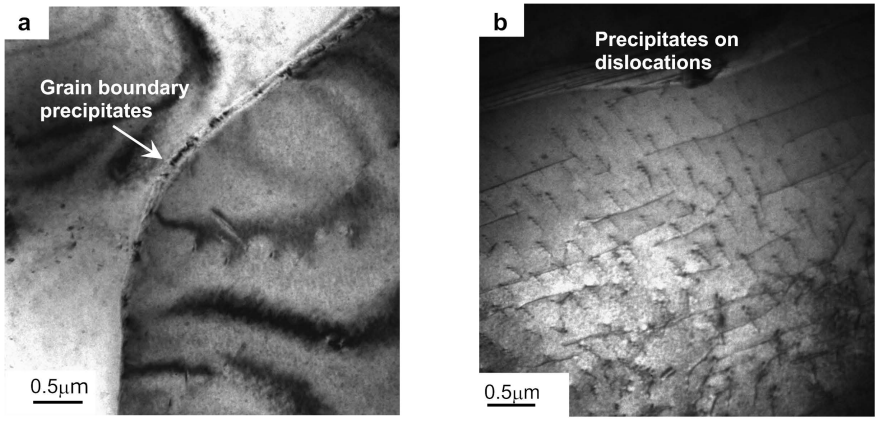

Figure 14. Bright field TEM micrographs illustrating; (a) grain boundary precipitation and (b) precipitation on dislocations - in Nb-microalloyed steels [6].

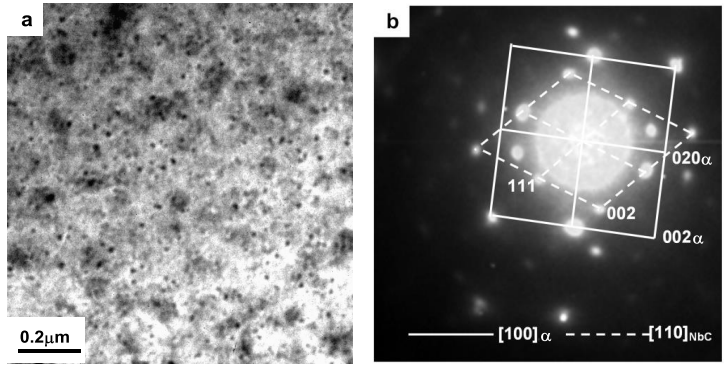

Figure 15. Bright field TEM micrograph illustrating; (a) fine-scale precipitation in the ferrite matrix and (b) corresponding SAD pattern analysis for the precipitate and the matrix - in Nb-microalloyed steels [6].

Table III. Precipitate Characteristics of Nb-microalloyed Steels

Properties	Nb-microalloyed Steels	
	Conventional Cooling Rate	Higher Cooling Rate
Mean particle size (d), nm	5.25 ± 3.5	7.5 ± 4.5
Mean inter-particle spacing, nm (50 measurements)	66 ± 37	50 ± 29
Particle density, (No. of particles/~ 0.5 μm^2)	280	320

The above results suggest that Nb-microalloyed steels experience strain-induced precipitation at grain boundaries and dislocations, while the fine precipitates in ferrite are formed during cooling. The precipitation of microalloying elements occurs during various stages of thermomechanical processing of steels. At soaking temperatures the microalloying element, Nb, is taken into solution depending on the limitation imposed by the solubility product. For carbide and nitride forming elements, the solubility in austenite at any given temperature depends on the C and N content of the steel. When the temperature is lowered during cooling, supersaturation of these solute elements increases and precipitation begins under favorable kinetic conditions. Deformation of austenite introduces lattice defects such as dislocations and vacancies that assist the diffusional process and control the precipitation kinetics. As a result, strain-induced precipitation occurs at the prior austenite grain boundaries or defects. The precipitate size range for effective precipitation hardening is ~5-20 nm [13,14]. These fine precipitates exhibited a Baker-Nutting orientation relationship (Figure 15(b)) with the ferrite matrix in Nb-microalloyed steels, which confirmed that the precipitation occurred in ferrite.

Strength-toughness Combination in Nb-microalloyed Steels

The microstructural parameters that influence toughness are ferrite grain size, degenerate pearlite, and acicular ferrite/bainitic ferrite. The finer cementite in degenerate pearlite as compared to conventional pearlite is expected to not only yield higher strength but also improve toughness because coarse pearlite deforms inhomogeneously with strain localized in narrow slip bands, whereas fine degenerate pearlite exhibits a uniform strain distribution during deformation [15]. A schematic diagram illustrating the nature of cementite platelets present in the lamellar pearlite and degenerate pearlite and its effect on plastic deformation is presented in Figure 16. Fine cementite particles also increase the work hardening rate by creating the strain gradient near the particles due to the formation of Orowan loops. The dislocations constituting the strain gradient are referred to as geometrically necessary dislocations [11,12]. Thus, the significant increase in toughness with cooling rate in Nb-microalloyed steels is related to the toughness enhancing phase, bainite.

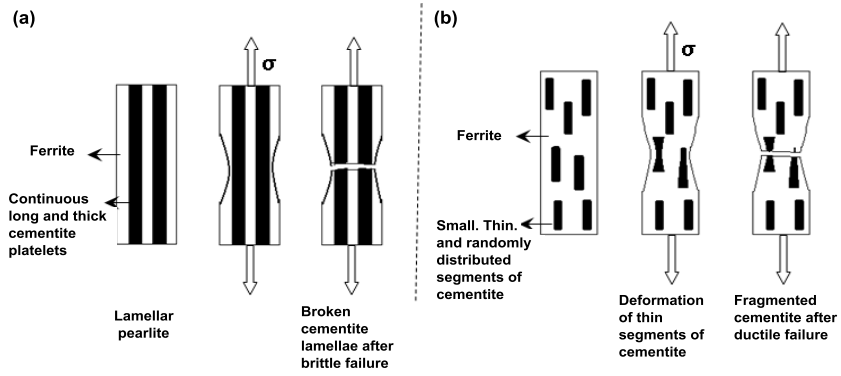

Figure 16. Schematic illustration of deformation of cementite in lamellar pearlite (a) and degenerate pearlite (b).

Conclusions

Nb as a microalloying element offers significant benefits in enhancing both the strength and toughness of medium and heavy sections for high-rise structures. The benefits include refinement in grain size, precipitation strengthening, promoting the desired microstructure and thus obtaining high strength-high toughness combinations. Nb, as a microalloying element, offers considerable flexibility in processing medium and heavy sections, in terms of entry/finish temperatures and cooling practice.

Acknowledgments

The author (Devesh Misra) gratefully acknowledges financial support of CBMM North America for the work presented here. Grateful thanks are also to Dr. D. Panda and Mr. T. Mannering for helpful discussions.

References

1. I. Gonzalez-Bequest, R. Kaspar and J. Richter, "Conditioning of Austenite by Hot Working of Microalloyed Forging Steels," *Steel Research*, 68 (2) (1997), 61-66.

2. Q. Yu et al., "Effect of Microcontent Nb in Solution on the Strength of Low Carbon Steels," *Materials Science and Engineering A*, 379 (1-2) (2004), 384-390.

3. S. Jansto, "Cost Effective Microalloy Structural Steel Balance of Process Metallurgy and Materials Engineering," *Proceedings of Materials Science and Technology (MS&T) 2008, International Symposium on Materials Engineering for Structural Applications,* October 5-9, 2008, 1289-1301.

4. L. Meyer, F. Heisterkamp and W. Muschenborn, "Columbium, Titanium and Vanadium in Normalized, Thermo-Mechanically Treated and Cold-Rolled Steels," *Micro Alloying 1975*, 153-167.

5. M. Piette et al., "Effect of 0-0.1% Nb Additions on Mechanical Properties of Plates Processed by Thermomechanically Controlled Processing and Accelerated Cooling," *Ironmaking and Steelmaking*, 28 (2) (2001), 175-179.

6. S. Shanmugam et al., "Impact Toughness and Relationship in Niobium and Vanadium Microalloyed Steels Processed with varied Cooling Rates to similar Yield Strength," *Materials Science and Engineering A,* 437 (2006), 436-445; "Effect of Cooling Rate on the Microstructure and Mechanical Properties of Nb Microalloyed Steels," *Material Science and Engineering A,* 460-461 (2007), 335-343.

7. Y. Ohmori and R.W.K. Honeycombe, "The Isothermal Transformation of Plain Carbon Austenite, Proceedings of ICSTIS (suppl.)," *Transactions Iron and Steel Institute of Japan*, 11 (1971), 1160-1165.

8. G. Krauss and S.W. Thompson, "Ferrite Microstructures in Continuously Cooled Low and Ultralow Carbon Steels," *Iron and Steel Institute of Japan International*, 35 (8) (1995), 937-945.

9. Y. Ohmori, "The Isothermal Decomposition of an Fe-C-B Austenite," *Transactions Iron and Steel Institute of Japan,* 11 (1971), 339-348.

10. T. Yamane et al., "Improvement of Toughness of Low Carbon Steels Containing Nitrogen by Fine Microstructure," *Journal of Materials Science*, 37 (18) (2002), 3875-3879.

11. R. Song, D. Ponge and D. Raabe, “Improvement of the Work Hardening Rate of Ultrafine Grained Steels Through Second Phase Particles,” *Scripta Materialia*, 52 (11) (2005), 1075-1080.

12. R. Song et al., “Microstructure and Crystallographic Texture of an Ultrafine Grained C Mn Steel and their Evolution during Warm Deformation and Annealing,” *Acta Materialia,* 53 (3) (2005), 845-858.

13. R.D.K. Misra et al., “Ultrahigh Strength Hot Rolled Microalloyed Steels: Microstructural aspects of Development,” *Material Science and Technology*, 17 (2001), 1119-1129.

14. R.R. Thridandapani et al, “Understanding Strength Toughness Combinations of Microalloyed Steels Processed for Large Structural Applications through Stereological Analysis,” *Proceedings of MS&T,* 2005, TMS, Volume 2 Pittsburgh, USA, 129.

15. H. Joung Sim, Y. Bum Lee and W.J. Nam, “Ductility of Hypo-eutectoid Steels with Ferrite Pearlite Structures,” *Journal of Material Science*, 39 (5) (2004), 1849-1851.